

Determining the ability of astaxanthin from *Haematococcus pluvialis* on the protection of skin in the mouse model

Quan Minh To^{1,4}, Nhan Dinh Tran¹, Truc Thi Thanh Vo², Thao Thu Huynh², Dieu Quang Tran¹, Trinh Nguyen Ai Ta¹, Bien Dinh Lai², Dung Hoang Nguyen^{3,4}, Long Thanh Le^{3,4*}

¹Faculty of Biology and Biotechnology, University of Science, Vietnam National University of Ho Chi Minh City, Hochiminh City, Vietnam

²Ho Chi Minh City of Food Industry, Hochiminh City, Vietnam

³Institute of Tropical Biology, Vietnam Academy of Science and Technology, Ho Chi Minh City, Vietnam

⁴Biotechnology Department, Graduate University of Science and Technology, Vietnam Academy of Science and Technology, Ha Noi, Vietnam

ARTICLE INFO

Article history:

Received on: January 14, 2021

Accepted on: March 27, 2021

Available online: July 10, 2021

Key words:

Astaxanthin, *Haematococcus pluvialis*, cell senescence, skin aging, hydrogen peroxide, ultraviolet irradiation

ABSTRACT

This study focuses on determining astaxanthin (AST)'s ability to prevent adverse effects of H₂O₂ and ultraviolet (UV) irradiation on cells and skin. A *Haematococcus pluvialis* strain, obtained from Vietnam, was used for AST extraction. It consists of free (4.4% ± 0.7%) and esterified form and accounts for 2.9% ± 0.5% dry weight. 3T3 cells were pre-treated with AST (1, 2.5, 5, 10 µg/ml) or commercial astaxanthin (10 µg/ml) for 24 hours prior to H₂O₂ treatment (200 µM, 90 minutes). The results showed that the AST protected 3T3 cells: reduction of mortality rate (16.08%–21.52%), senescence-associated β-galactosidase—positive cells (28.9%–40.8%), and maintenance of cell proliferation, morphology. AST 5 µg/ml is the optimal concentration in this experiment. *Mus musculus* var. *Albino* was treated with a daily dose of topical AST (20 or 200 µg/ml) and UV irradiation for 6 weeks. The results showed that AST reduced wrinkles and retained mouse skin's physiology that closed to the control group. AST 20 µg/ml was the best effective concentration in this experiment. In conclusion, AST has been shown to have the ability to protect fibroblasts, skin from the adverse effects of H₂O₂, UV irradiation.

1. INTRODUCTION

Astaxanthin (AST) (3,3-dihydroxy-β,β-carotene-4,4-dione), a red xanthophyll carotenoid, has been acknowledged as one of the most effective antioxidants. AST consists of the two β-ionone-type rings at both ends and one polyene chain in the structure; hence AST easily attaches to the cell or organelle membrane (Fig. 1) [1,2]. Hence, AST can protect cells by neutralizing or quenching free radicals produced inside or outside the cells [3,4]. *Haematococcus pluvialis*, unicellular microalgae, is the best natural, commercial source of AST [3]. AST is commonly absorbed through the oral route to ameliorate Parkinson's disease, stroke, high cholesterol, liver diseases, aging [1,3,5]. In the cosmetic field, AST was used as an anti-aging agent to protect skin from adverse effects of ultraviolet (UV) irradiation and reactive oxygen species (ROS) [6,7]. UV irradiation and

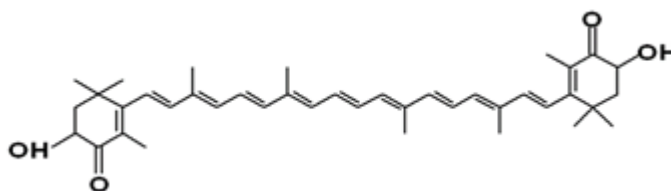


Figure 1: Structure of astaxanthin [3].

ROS can break down DNA in skin cells, the extracellular matrix (ECM), such as collagen, elastin, and up-regulate enzymes that degrade skin ECM, such as matrix metalloproteinase-1 (MMP-1), neutral endopeptidase (NEP). These modifications lead to cell death, senescence, and aging skin [8–11]. AST was proved to prevent DNA damage, reduce the expression, and activity of MMP-1 and NEP in UV-induced fibroblast *in vitro* [12,13]. However, the protective ability of AST against ROS on fibroblast is limited. Currently, AST was applied frequently as an oral nutritional supplement; yet studies in topical application of AST in the cosmetic field have been neglected [6,7]. In this study, we

*Corresponding Author

Long Thanh Le, Institute of Tropical Biology, Vietnam Academy of Science and Technology, Ho Chi Minh City, Vietnam.
E-mail: longlt@itb.ac.vn

aim to extract AST from a new *H. pluvialis* strain isolated in Vietnam and determine its protective effects against ROS (H_2O_2) on fibroblasts (*in vitro*) and against UV irradiation on mouse skin (*in vivo*).

2. MATERIALS AND METHODS

2.1. Astaxanthin Extraction

The green algae *Haematococcus pluvialis* was cultivated in 750-ml sterilized glass columns containing 450 ml of modified BG-11 medium. The flasks were illuminated at $40 \mu\text{mol}\cdot\text{m}^{-2}\cdot\text{s}^{-1}$ of white light (Philips, TLD 18W) with a dark: light cycle of 12 hours:12 hours, 22°C and continuously aerated by the bubbling air. Cell number was counted by a hemacytometer cell counting chamber. For astaxanthin (AST) induction, logarithmic cells were incubated in BG-11 with nitrogen deficiency at high light intensity ($170 \mu\text{mol}\cdot\text{m}^{-2}\cdot\text{s}^{-1}$) with a light: dark cycle of 24:0 for 2–3 weeks [14]. Astaxanthin was extracted according to Sarada [15] with some modifications. Freeze-dried algae were treated by HCl 2 M for 2 minutes, ground, and extracted in acetone. AST concentration was evaluated by High-performance liquid chromatography (HPLC) [16].

2.2. ABTS Assay

The ABTS radical solution was prepared by oxidation of ABTS (7 mM) by $K_2S_2O_8$ (2.45 mM). This solution was incubated for 14–16 hours in dark and then diluted in ethanol to obtain a working solution that has an absorbance of 0.7 ± 0.02 at the wavelength of 734 nm. Next, 80 μl of AST solution in different concentrations was mixed with ABTS working solutions and the OD values at 734 nm were recorded after 60 minutes. Trolox was used as a positive control. The inhibition percentage was calculated as the following formulation: Percentage (%) = $[1 - (A_{\text{final}}/A_{\text{initial}})] \times 100\%$, where A_{initial} and A_{final} are the absorbances at 734 nm at the beginning and final step [17,18].

2.3. Tyrosine Inhibition Test

Astaxanthin in different concentrations was added to wells of 96-well plates (50 μl /well), followed by adding 50 μl tyrosinase (25 U/well). The mixture was stored at room temperature for 15 minutes, and then supplemented with L-DOPA (100 μl) and left at room temperature. After 15 minutes, OD values at 492 nm were recorded. The percentage of inhibition was evaluated as the following formula: %inhibition = $[(\text{OD}_{\text{blank-A}} - \text{OD}_{\text{blank-B}}) - (\text{OD}_{\text{sample-A}} - \text{OD}_{\text{sample-B}})] / (\text{OD}_{\text{blank-A}} - \text{OD}_{\text{blank-B}}) \times 100$ where $\text{OD}_{\text{blank-A}}$, $\text{OD}_{\text{blank-B}}$ is the absorbance of blank after and before test, $\text{OD}_{\text{sample-A}}$, $\text{OD}_{\text{sample-B}}$ is the absorbance of the sample after and before test [17].

2.4. In Vitro Cytotoxicity Assay

3T3 cells were cultured in cell culture medium containing 90% DMEM/F12, 10% fetal bovine serum (FBS), 1% antibiotics in 37°C , 5% CO_2 . The cells were seeded into a 96-wells plate at a density of 4×10^3 cells/well. After 24 hours, the cells were treated with AST in the range of 1–10 $\mu\text{g}/\text{ml}$ (5 wells/group), the final DMSO concentration, which was used to dissolve AST, was

0.5%. Cell culture medium containing 0.5% DMSO was used as a control. After 1 day, cytotoxicity was evaluated by WST-1 assay according to the manufacturer's instruction [19]. OD values were recorded at wavelength of 440 nm.

2.5. In Vitro Evaluation of the Protective Ability of AST against H_2O_2 -Induced Oxidative Stress

3T3 cells were pre-treated with various AST concentrations (1, 2.5, 5, or 10 $\mu\text{g}/\text{ml}$) for 12 hours before the H_2O_2 treatment. H_2O_2 -induced oxidative stress in fibroblast was performed according to Yokozawa et al. [20] with some modifications. First, 3T3 cells were seeded on a 96-wells plate at a density of 10×10^3 cells/well. One day later, cells were pre-treated with AST 1, 2.5, 5, and 10 $\mu\text{g}/\text{ml}$ or commercial AST (trAST) (10 $\mu\text{g}/\text{ml}$) for 12 hours, cell culture medium containing 0.5% DMSO was used as a H_2O_2 control. Next, all cells (AST, trAST, and H_2O_2 control groups) were challenged by 200 μM H_2O_2 dissolved in DMEM/F12 5% FBS for 90 minutes. Then, the medium was replaced. Viable cells were examined by Hemocytometer and seeded on a 4-well plate with a concentration of 3×10^4 viable cells/well. Four days later, WST-1 assay, DAPI/ phalloidin staining, and senescence-associated β -galactosidase (SA-gal) staining were performed to test cell viability, cell nucleus area, and SA-gal expression. Cell culture medium containing 0.5% DMSO (non-treated H_2O_2) was used as a blank control group (Table 1).

2.6. In Vivo Evaluation of the Protective Ability of AST against UV-Induced Skin Lesion

AST was dissolved in commercial Sacha Inchi oil to achieve the concentrations of 20 or 200 $\mu\text{g}/\text{ml}$. *Mus musculus* var. *Albino* mice (age of 5–6 weeks, 30–35 g) were purchased from Pasteur Institute of Hochiminh city 1 week before the experiments. The mice were housed at 25°C with a dark: light cycle of 12 hours:12 hours. The study was approved by the Animal Care and Use Committee (ACUCUS) of University of Science, Vietnam National University of Hochiminh city (approval number 1170B/KHTN-ACUCUS). The experiment was divided into five groups that belong to Table 1. UV radiation was performed using a UV lamp (Exo Terra, UVB 150, 25W), which gives the full solar spectrum with high UVB output. The dorsal skin of the mice was shaved and irradiated by UV light. UVB intensity was 100 mJ/cm^2 per time for weeks 1–2 (three times/week), 200 mJ/cm^2 per time for weeks 3–4 (three times/week), and 300 mJ/cm^2 per time for weeks 5–6 (three times/week) [21]. After 6 weeks, wrinkle formation was evaluated based on the grading scale of Rumjhum Agrawal, and skin was stained by Trichrome staining [22]. In AST groups, dorsal skin was topically treated daily with AST (20 or 200 $\mu\text{g}/\text{ml}$) 8 hours before UV irradiation as the above method.

Table 1: Groups in experiment of AST ability against H_2O_2 treatment.

	Blank	Control	AST	trAST
AST concentration in culture medium containing 0.5% DMSO ($\mu\text{g}/\text{ml}$)	None	None	1 or 2.5 or 5	5
H_2O_2 treatment	None	Yes	Yes	Yes

2.7. Statistical Analysis

Statistical analysis was performed using one-way analysis of variance with SigmaPlot software where $p < 0.05$ was considered to be statistically significant.

3. RESULTS

3.1. Astaxanthin Extraction

Under low light intensity condition ($40 \mu\text{mol}\cdot\text{m}^{-2}\cdot\text{s}^{-1}$), *H. pluvialis* cells predominantly existed in green motile zoospore stage with $20\text{--}30 \mu\text{m}$ in diameter and 2 flagella. The cell concentration rapidly reached a peak of 9.5×10^5 cells/ml after 14–18 days of culture with inoculation of 1×10^5 cells/ml. Under unfavorable conditions: high light intensity ($170 \mu\text{mol}\cdot\text{m}^{-2}\cdot\text{s}^{-1}$) and nitrogen deficiency, the algal cells rapidly changed to the encystment stage. They begin to lose flagella, expand cell volume, and thicken the cell wall (palmella stage). After 7–10 days of induction, AST occurred in the center of the cell and rapidly occupied the entire cytoplasm. Most of the cells developed into aplanospores after 28–35 days of induction. HPLC results showed that AST concentration is $2.9\% \pm$

0.5% of dry weight and free AST accounted for $4.4\% \pm 0.7\%$ total AST (Fig. 2).

3.2. ABTS Assay

ABTS assay was used for determining the activity of antioxidants which reduce radical ABTS and decolorize its color. After 60 minutes of incubation, ABTS working solution changed to colorless (incubated with Trolox) or light orange (incubated with AST). The inhibition percentage of Trolox and AST was shown in Figure 3. IC_{50} value of Trolox was $604.8 \pm 9.5 \mu\text{M}$. The results showed that AST had ABTS scavenging activity in the range of $12.5\text{--}160 \mu\text{g/ml}$ with an IC_{50} value of $148.02 \mu\text{g/ml}$ and TEAC value was $0.126 \text{ mmol Trolox/g extract}$ (Fig. 3).

3.3. Tyrosinase Inhibition Test

Tyrosinase catalyzes tyrosine to dopaquinone which polymerized to dark pigment having the maximum absorbance at a wavelength of 492 nm [23]. The results showed that the AST could inhibit tyrosinase activity with IC_{50} of $120.4 \mu\text{g/ml}$ extraction and the IC_{50}

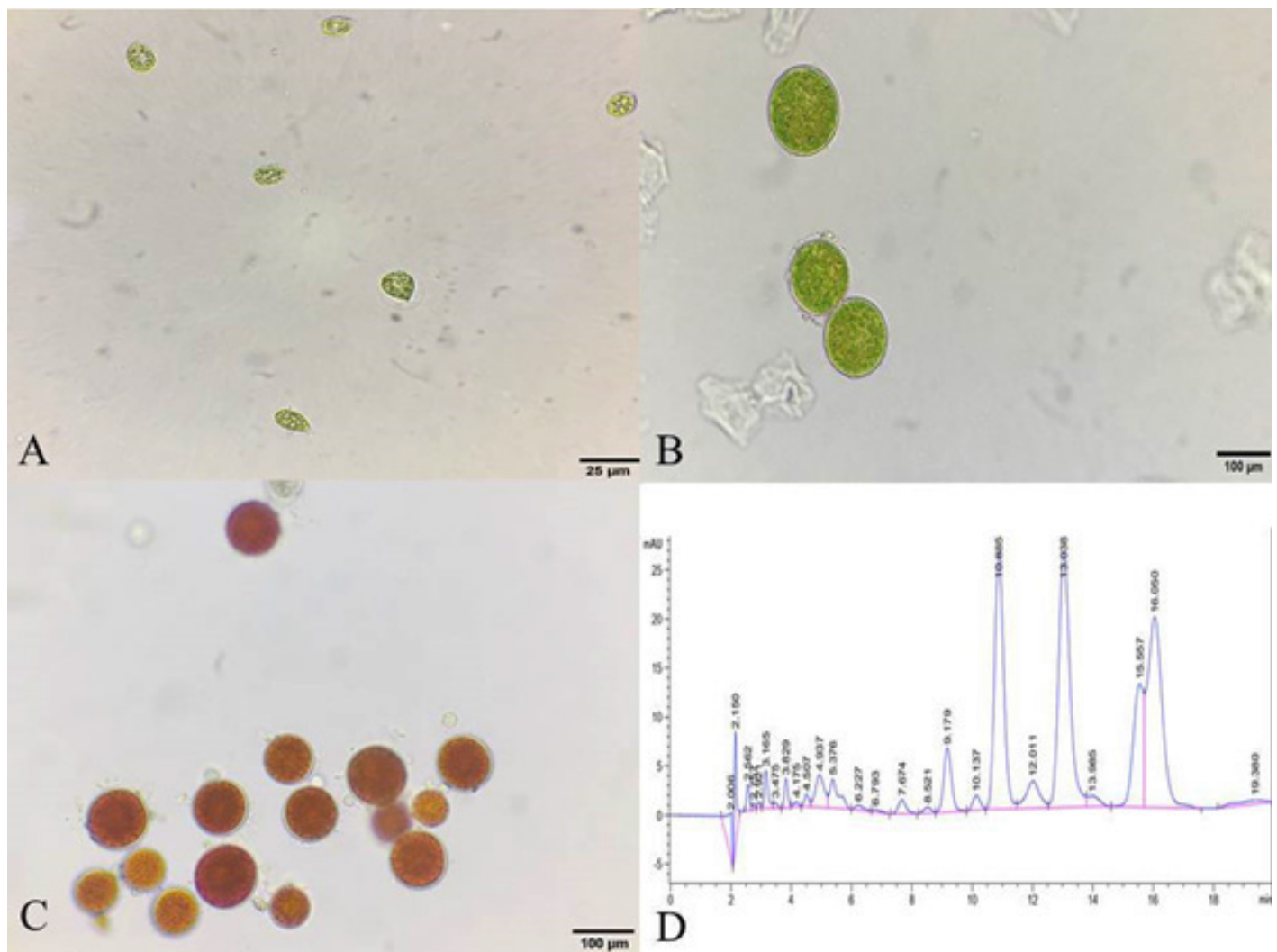


Figure 2: Astaxanthin from *H. pluvialis*. (A) Motile macrozooids ($\times 200$), (B) Palmella ($\times 100$), (C) Aplanospores ($\times 100$) and (D) HPLC of AST extraction.

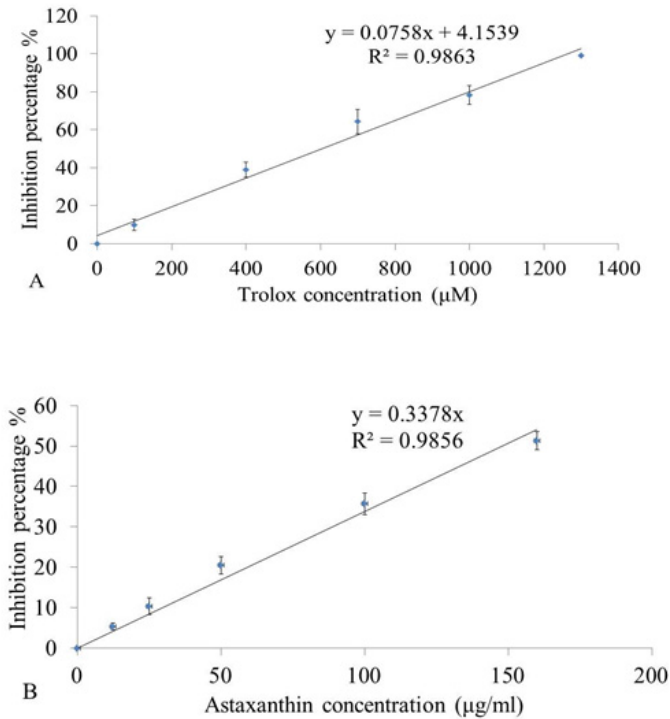


Figure 3: The results of ABTS assay. (A) Trolox and (B) AST.

Table 2: Groups in experiment of AST ability against UV irradiation.

	Control	UV	Oil	AST 20	AST 200
Topical treatment	None	None	Saccha Inchi oil	AST 20 μg/ml	AST 200 μg/ml
UV irradiation	None	Yes	Yes	Yes	Yes

value of kojic acid (the control) was 25.6 μg/ml (180.9 μM). The results showed AST could inhibit tyrosinase and less potent than kojic acid.

3.4. Cytotoxicity Test *In Vitro*

3T3 cells were exposed to the medium supplemented with AST (0, 1, 5, or 10 μg/ml) ($n = 5$). OD values of WST-1 assay were shown in Table 2. OD values of all groups were not statistically different ($p < 0.05$) (Table 2). Moreover, after 1 day, morphological alterations and cell detachment were not observed, 3T3 cells retained fibroblast-like shape with elongate morphology (Fig. 4). It was concluded that AST in the range of 1–10 μg/ml was not cytotoxic to fibroblast cells.

3.5. *In Vitro* Evaluation of Protection Activity of AST

The experiment was performed in Table 1. In the control group, soon after the stress, the mortality rate increased significantly from 2.5% ± 0.4% (blank group) to 25.4% ± 3.5% of cells ($p < 0.05$) (Fig. 5A). Next 4 days, the OD values did not increase, it was comparable to day 1 ($p > 0.05$). The morphological alterations were observed on day 4th: the enlargement of cell nuclear size (430.6 ± 81.8 μm²) and cell size (data not shown) (Fig. 6B). Moreover, the percentage of SA-gal-expressed cells (a biomarker of cell senescence) in this group was 61.9 ± 7.5 which significantly

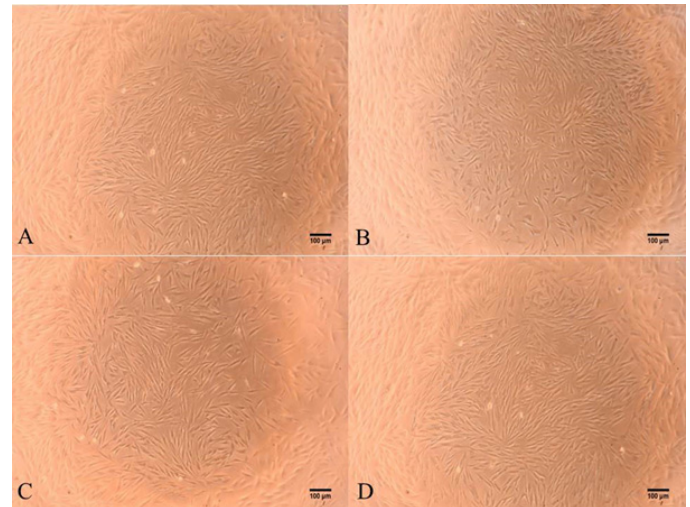


Figure 4: 3T3 cells after 1 day treatment with AST. (A) Control (×100), (B–D) AST 10, 25, and 50 μg/ml (×100).

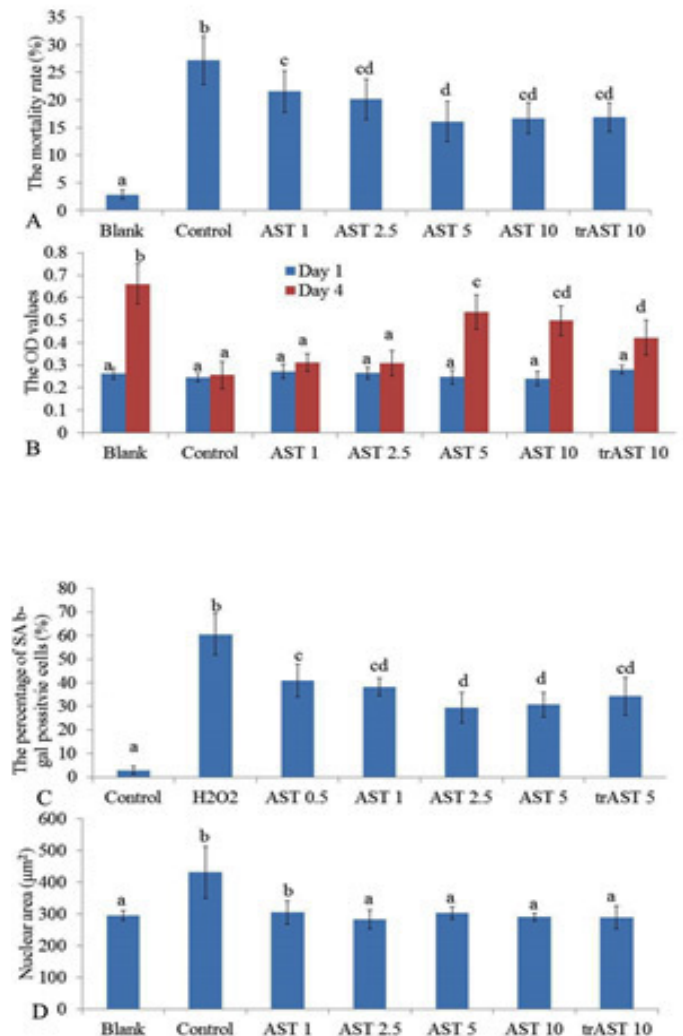


Figure 5: Graphs show protective ability of AST on fibroblast. (A) cell mortality, (B) WST-1 assay, and (C) SA-b Gal expression. (^{a,b,c,d}: significant difference).

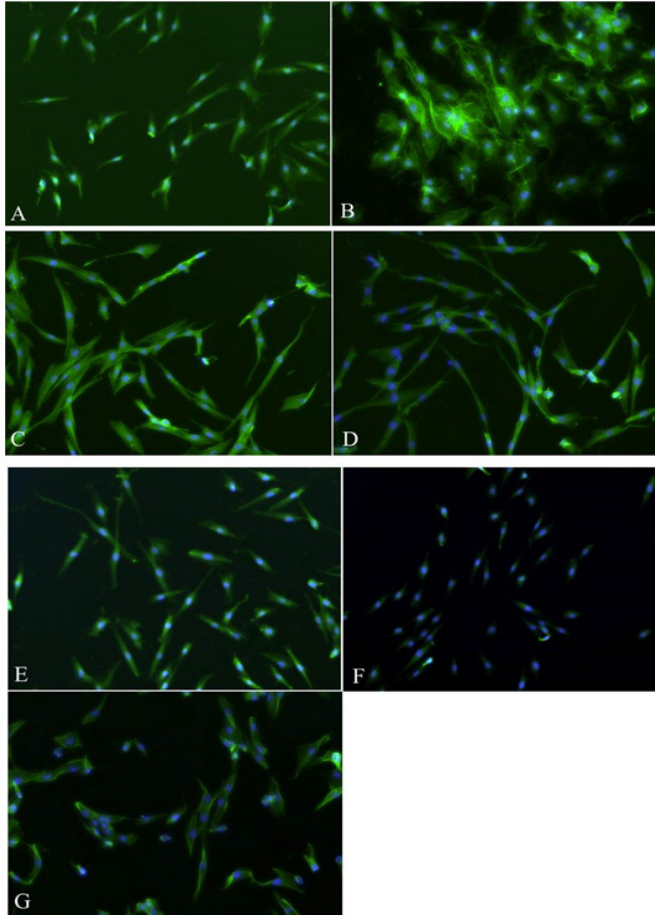


Figure 6: The cells were stained with DAPI/phalloidin blue. (A) Normal cells, (B) H₂O₂ treated cells, (C–F) AST 1, 2.5, 5, and 10 µg/ml, and (G) 10 µg/ml (×100).

Table 3: OD value of WST-1 assay in cytotoxicity test.

AST concentration	0 µg/ml (control)	1 µg/ml (AST)	5 µg/ml (AST)	10 µg/ml (AST)
OD value	0.43 ± 0.11 ^a	0.42 ± 0.07 ^a	0.41 ± 0.15 ^a	0.43 ± 0.09 ^a

^aNot significant difference.

higher than the blank and AST groups ($p < 0.05$) (Fig. 7). These results showed that H₂O₂ caused cell death accompanied by cell senescence, including the inhibition of cell proliferation, the increase of nuclear area, cell size, and SA b-Gal expression.

In the AST group, the cells were sequentially treated with AST (1, 2.5, 5, and 10 µg/ml) and H₂O₂. The death rate in all AST groups was lower than the control group ($p < 0.05$). The WST-1 assay showed that OD values in group AST 1, 2.5 rose slightly on day 4th compared to day 1st ($p > 0.05$) while OD values in group AST 5, 10 on day 4th was higher than day 1st ($p < 0.05$). The results of DAPI/phalloidin staining showed cells in all AST groups retained their initial shape: spindle-like morphology with a smaller nuclear area than control ($p < 0.05$). The ratio of SA-gal-positive cells was lower than the control group ($p < 0.05$) (Figs. 5C and 7). Based on these results, we concluded that AST prevented the adverse effects of H₂O₂-induced oxidative stress in a dose-dependent manner.

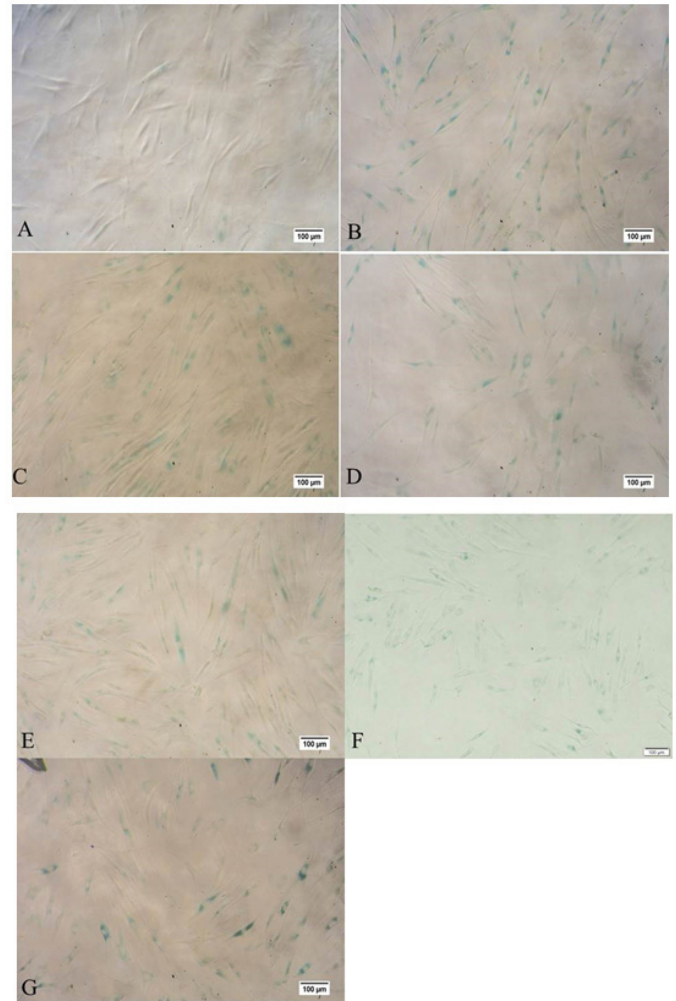


Figure 7: SA-b Gal expression of the cells. (A) Normal cells, (B) H₂O₂-treated cells, (C–F) AST 1, 2.5, 5, and 10 µg/ml, and (G) 10 µg/ml (×100).

Between the various concentrations, AST 5–10 gives the best effect in protecting the fibroblast cells in this experiment.

3.6. *In Vivo* Evaluation of the Protective Ability of AST against UV-Induced Skin Lesion

To determine the capacity to protect skin from UV damage, AST is topically applied on dorsal skin before UV irradiation. The visible appearance of the dorsal skin changed after 6 weeks of UV irradiation. The skin of all mice lost its color, became dry and rough. Moreover, some deep wrinkles perpendicular to the spine had appeared since week 4 (Fig. 8 and Table 4). In AST groups, skin remained smooth and reddish color, fine striation appeared (Fig. 8 and Table 4) (score was 4.3 ± 0.5). There is no significant difference between the wrinkle score of mice in AST 20 and 200 µg/ml (2.3 ± 0.5 , 2.5 ± 0.5). Trichrome staining was carried out to verify the histological structure of the skin. After 6 weeks, there is a considerable increase in epithelium thickness in the UV group compared to the control group (42.2 ± 8.9 µm, 20.5 ± 4.5 µm). In AST groups (20 or 200 µg/ml), the thickness of these groups was smaller than the UV group and higher than the control group (28.9

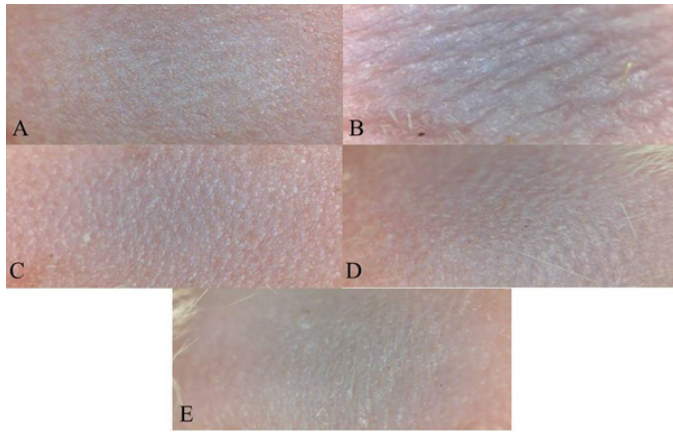


Figure 8: Skin surface at week 6th post-treatment. (A) Control, (B), UV group, (C) oil, (D and E) AST 20, 200 µg/ml.

Table 4: Results of groups in skin protection from UV damage.

Group	Control	UV	Oil	AST 20	AST 200
Wrinkle score	0.7 ± 0.5 ^a	4.3 ± 0.5 ^b	3.4 ± 0.7 ^c	2.3 ± 0.5 ^d	2.5 ± 0.5 ^d
Epithelial layer (µm)	20.5 ± 4.5 ^a	42.2 ± 8.9 ^b	36.0 ± 5.9 ^b	28.9 ± 3.1 ^c	32.2 ± 4.9 ^{b,c}

(^{a,b,c,d} Significant difference between groups in the same row).

± 3.1 µm, 32.2 ± 4.9 µm) ($p < 0.05$) (Fig. 9 and Table 4). There is no significant difference between the epithelial layer of mice in AST 20 and 200 µg/ml ($p > 0.05$). These results showed that AST ameliorated UV-induced lesions on mouse skin.

4. DISCUSSION AND CONCLUSION

AST is a powerful antioxidant and adheres easily to the membranes of cells, mitochondrial, nucleus [2,4]. Therefore, AST could prevent the harmful effects of free radicals produced in the intracellular and extracellular environment. *Haematococcus pluvialis* is one of the best natural sources of AST that contains the maximum AST concentration of 5% dry weight [6,24]. In Vietnam, Dang Thi Diem Hong is the first to isolate and culture *H. pluvialis*. This strain, obtained from the North of Vietnam, can reach the concentration of 0.95×10^6 cells/ml in a modified RM medium after 15 days of inoculation [25]. In this study, we aimed to investigate its ability to protect skin against the harmful effects of H₂O₂ and UV irradiation. The results showed that AST occupied 2.9% dry weight and existed in two different forms: free (4.4%) and esterified, in which ester form is the predominant part (data not shown). The ABTS assay shows that AST is a potent antioxidant and its TEAC value was 0.126 mmol Trolox/g extract closed to Zuluaga's et al. [18]. Moreover, AST could reduce tyrosinase activity, which less effective than kojic acid. This result is similar to Chintong et al. [19]. Therefore, AST could be used as a skin-lightening agent.

UV irradiation and ROS are the most harmful factors to the skin. UV, composed of predominant UVA and UVB, can break down DNA double helix and create abnormal covalent bonds or produce ROS [26,27]. ROS is generated in normal metabolic processes or cellular reactions. Its level depends on age and is accelerated by UV induction [28,29]. Many kinds of research prove the protective

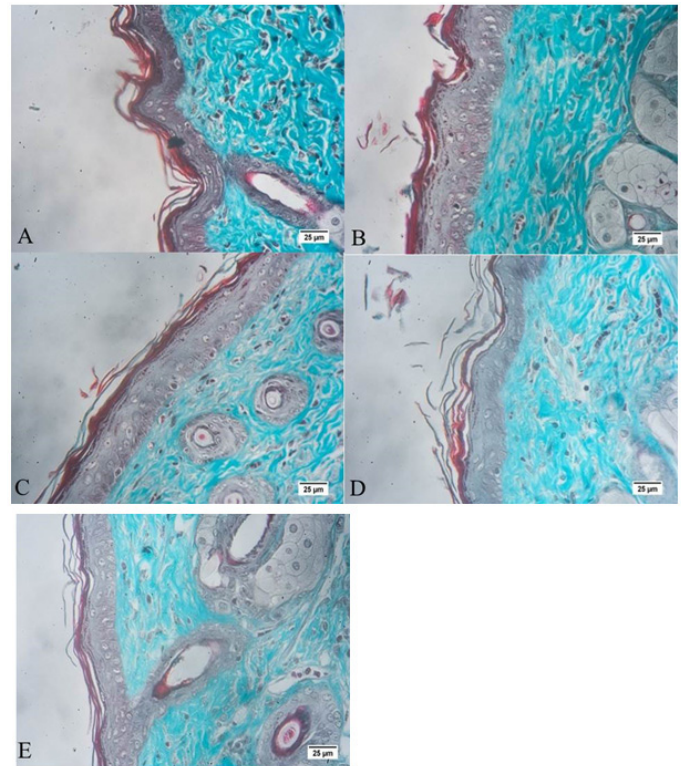


Figure 9: Trichrome staining of mouse skin at week 6th post-treatment. (A) Control, (B) UV group, (C) Saccha Inchi oil, and (D and E) AST 20, 200 µg/ml (×200).

effect of AST on fibroblast against UV irradiation on fibroblasts *in vitro* [12,13,30]. However, little research checks on its ability to prevent oxidative stress into fibroblast. H₂O₂, a powerful oxidizing agent, is usually used in senescent experiments [20,31]. The results showed that H₂O₂ triggered cell death (approximate 25% of cells), inhibited proliferation, and induced cell senescence. Moreover, over half of the cells expressed SA b-gal, a gold marker for cell senescence [31,32]. These results showed that H₂O₂ induced oxidative stress damage on fibroblasts [31,33]. In experiment groups, cells were pre-treated with AST (1–10 µg/ml) before H₂O₂ treatment. The results showed that AST reduced cell death rate, maintained cell proliferation, and suppressed SA b-gal expression. It was concluded that AST (1–10 µg/ml) could defend fibroblast against H₂O₂-induced oxidative stress, in which the 5 µg/ml was the best effective concentration.

Skin lesions on *Mus musculus* var. *Albino* was caused by UV irradiation, according to Kim et al. [21] with some modifications. We used the Extro UVB 150 lamp, which gives a high output UVB similar to the solar spectrum in deserts. The amount of UV irradiation was calculated based on the UVB intensity of this lamp measured by a UVB meter. After 6 weeks of treatment, some skin aging signs appeared, and the skin surface changed to be rough, sagging, and had many deep and shallow wrinkles. In this study, we want to examine AST as a topical skincare product that can be used one time a day (before sleeping). Hence, AST (20 or 200 µg/ml) was applied on the dorsal skin 8 hours before UV irradiation. The results showed the mouse skin retained initial characteristics, including smooth, reddish, and had many shallow wrinkles. So,

AST (20 or 200 µg/ml) ameliorated UV-induced skin lesions. We concluded that AST 20 µg/ml was the best effective concentration in this experiment.

5. CONCLUSION

AST was successfully extracted from *H. pluvialis* isolated in Vietnam. AST is a potent antioxidant that can prevent dangerous impacts from H₂O₂ and UV irradiation on the skin.

6. FINANCIAL SUPPORT

The study was supported by The Youth Incubator for Science and Technology Program, managed by Youth Development Science and Technology Center - Ho Chi Minh Communist Youth Union and Department of Science and Technology of Ho Chi Minh City, the contract number is "32/2019/HD-KHCN-VU".

AUTHOR CONTRIBUTIONS

All authors made substantial contributions to conception and design, acquisition of data, or analysis and interpretation of data; took part in drafting the article or revising it critically for important intellectual content; agreed to submit to the current journal; gave final approval of the version to be published; and agree to be accountable for all aspects of the work. All the authors are eligible to be an author as per the international committee of medical journal editors (ICMJE) requirements/guidelines.

CONFLICTS OF INTEREST

The authors report no financial or any other conflicts of interest in this work.

ETHICAL APPROVALS

This study does not involve experiments on animals or human subjects.

PUBLISHER'S NOTE

This journal remains neutral with regard to jurisdictional claims in published institutional affiliation.

REFERENCES

1. Pereira CPM, Souza ACR, Vasconcelos AR, Prado PS, Name JJ. Antioxidant and antiinflammatory mechanisms of action of astaxanthin in cardiovascular diseases (Review). *Int J Mol Med* 2020;47(1):37–48.
2. Lim KC, Yusoff FM, Shariff M, Kamarudin MS. Astaxanthin as feed supplement in aquatic animals. *Rev Aquac* 2018;10(3):738–73.
3. Ambati RR, Phang SM, Ravi S, Aswathanarayana RG. Astaxanthin: sources, extraction, stability, biological activities and its commercial applications—a review. *Mar Drugs* 2014;12(1):128–52.
4. Kidd P. Astaxanthin, cell membrane nutrient with diverse clinical benefits and anti-aging potential. *Altern Med Rev* 2011;17(4):355–64.
5. Brotosudarmo THP, Limantara L, Setiyono E, Heriyanto. Structures of astaxanthin and their consequences for therapeutic application. *Int J Food Sci* 2020;2020:1–12.
6. Davinelli S, Nielsen M, Scapagnini G. Astaxanthin in skin health, repair, and disease: a comprehensive review. *Nutrients* 2018;10(4):522.
7. Higuera-Ciapara I, Félix-Valenzuela L, Goycoolea FM. Astaxanthin: a review of its chemistry and applications. *Crit Rev Food Sci Nutr* 2006;46(2):185–96.
8. Bosset S, Bonnet-Duquennoy M, Barre P, Chalon A, Kurfurst R, Bonte F, Schnebert S, Le Varlet B, Nicolas JF. Photoageing shows histological features of chronic skin inflammation without clinical and molecular abnormalities. *Br J Dermatol* 2003;149(4):826–35.
9. Kim M, Park HJ. Molecular mechanisms of skin aging and rejuvenation, in molecular mechanisms of the aging process and rejuvenation. 2016, IntechOpen, United Kingdom.
10. Rabe JH, Mamelak AJ, Mcelgunn PJ, Morison WL, Sauder DN. Photoaging: mechanisms and repair. *J Am Acad Dermatol* 2006;55(1):1–19.
11. Tominaga K, Hongo N, Fujishita M, Takahashi Y, Adachi Y. Protective effect of astaxanthin on skin deterioration. *J Clin Biochem Nutr* 2017;61(1):33–9.
12. Lyons NM, NM O'brien. Modulatory effects of an algal extract containing astaxanthin on UVA-irradiated cells in culture. *J Dermatol Sci* 2002;30(1):73–84.
13. Camera E, Mastrofrancesco A, Fabbri C, Daubrawa F, Picardo M, Sies H, et al. Astaxanthin, canthaxanthin and beta-carotene differently affect UVA-induced oxidative damage and expression of oxidative stress-responsive enzymes. *Exp Dermatol* 2009; 18(3):222–31.
14. Wong YK. Effects of light intensity, illumination cycles on microalgae *Haematococcus Pluvialis* for production of astaxanthin. *J Mar Biol Aquaculture* 2016;2(2):1–6.
15. Sarada R. An efficient method for extraction of astaxanthin from green alga *Haematococcus pluvialis*. *J Agric Food Chem* 2006;54:7585–8.
16. Su F, Xu H, Yang N, Liu W, Liu J. Hydrolytic efficiency and isomerization during de-esterification of natural astaxanthin esters by saponification and enzymolysis. *Electron J Biotechnol* 2018;34:37–42.
17. Chintong S, Phatvej W, Rerk-Am U, Waiprib Y, Klaypradit W. *In vitro* antioxidant, antityrosinase, and cytotoxic activities of astaxanthin from shrimp waste. *Antioxidants (Basel)* 2019;8(5):128.
18. Zuluaga M, Barzegari A, Letourneur D, Gueguen V, Pavon-Djavid G. Oxidative stress regulation on endothelial cells by hydrophilic astaxanthin complex: chemical, biological, and molecular antioxidant activity evaluation. *Oxid Med Cell Longev* 2017;2017:8073798.
19. Chintong S, Phatvej W, Rerk-Am U, Waiprib Y, Klaypradit W. *In vitro* antioxidant, antityrosinase, and cytotoxic activities of astaxanthin from shrimp waste. *Antioxidants (Basel)* 2019;8(5):1–11.
20. Yokozawa T, Satoh A, Kim YJ. Modulation of oxidative stress by proanthocyanidin in H₂O₂-exposed human diploid fibroblast cells. *Biosci Biotechnol Biochem* 2013;77(10):2056–60.
21. Kim HN, Gil CH, Kim YR, Shin HK, Choi BT. Anti-photoaging properties of the phosphodiesterase 3 inhibitor cilostazol in ultraviolet B-irradiated hairless mice. *Sci Rep* 2016;6(1):1–10.
22. Agrawal R, Kaur IP. Inhibitory effect of encapsulated curcumin on ultraviolet-induced photoaging in mice. *Rejuvenation Res* 2010;13:397–410.
23. Ramsden CA, Riley PA. Tyrosinase: the four oxidation states of the active site and their relevance to enzymatic activation, oxidation and inactivation. *Bioorg Med Chem* 2014;22(8):2388–95.
24. Shah MM, Liang Y, Cheng JJ, Daroch M. Astaxanthin-producing green microalga *Haematococcus pluvialis*: from single cell to high value commercial products. *Front Plant Sci* 2016;7:1–28.
25. Hong DD. Combined effects of nitrate concentration and illumination conditions on the growth of microalga *Haematococcus pluvialis*. *Tap chi Sinh Học* 2012;34(4):493–9.
26. De Jager TL, Cockrell AE, Du Plessis SS. Ultraviolet light induced generation of reactive oxygen species. *Adv Exp Med Biol* 2017;996:15–23.
27. Rastogi RP, Singh SP, Incharoensakdi A, Häder DP, Sinha RP. Ultraviolet radiation-induced generation of reactive oxygen species, DNA damage and induction of UV-absorbing compounds in the cyanobacterium *Rivularia* sp. HKAR-4. *S Afr J Bot* 2014;90:163–9.
28. Liebel F, Kaur S, Ruvolo E, Kollias N, Southall MD. Irradiation of skin with visible light induces reactive oxygen species and matrix-degrading enzymes. *J Invest Dermatol* 2012;132(7):1901–7.

29. Rinnerthaler M, Bischof J, Streubel MK, Trost A, Richter K. Oxidative stress in aging human skin. *Biomolecules* 2015;5(2):545–89.
30. Chou HY, Lee C, Pan JL, Wen ZH, Huang SH, Lan CW, et al. Enriched astaxanthin extract from *Haematococcus pluvialis* augments growth factor secretions to increase cell proliferation and induces MMP1 degradation to enhance collagen production in human dermal fibroblasts. *Int J Mol Sci* 2016; 17(6):955.
31. Kiyoshima T, Enoki N, Kobayashi I, Sakai T, Nagata K, Wada H, et al. Oxidative stress caused by a low concentration of hydrogen peroxide induces senescence-like changes in mouse gingival fibroblasts. *Int J Mol Med* 2012;30(5):1007–12.
32. Morgunova GV, Kolesnikov AV, Klebanov AA, Khokhlov AN. Senescence-associated β -galactosidase—a biomarker of aging, DNA damage, or cell proliferation restriction? *Moscow Univ Biol Sci Bull* 2015;70(4):165–7.
33. Park WH. H₂O₂ inhibits the growth of human pulmonary fibroblast cells by inducing cell death, GSH depletion and G1 phase arrest. *Mol Med Rep* 2013;7(4):1235–40.

How to cite this article:

To QM, Tran ND, Vo TTT, Huynh TT, Tran DQ, Ta TNA, Lai BD, Nguyen DH, Le LT. Determining the ability of astaxanthin from *Haematococcus pluvialis* on the protection of skin in the mouse model. *J Appl Biol Biotech* 2021; 9(04):85–92.